Systematic study of the impact of MOF densification into tablets on textural and mechanical properties

J. Dhainaut, C. Avci-Camur, J. Troyano, A. Legrand, J. Canivet, I. Imaz, D. Maspoch, H. Reinsch, D. Farrusseng

Systematic study of the impact of MOF densification into tablets on textural and mechanical properties

J. Dhainaut,[a] C. Avci-Camur,[b] J. Troyano,[b] A. Legrand,[b] J. Canivet,[a] I. Imaz,[b] D. Maspoch,[b] H. Reinsch [c], and D. Farrusseng[a]

Four different Metal-Organic Framework powders (UiO-66, UiO-66-NH_2, UiO-67, HKUST-1) were shaped into tablets. The effect of the applied pressure on porous properties, mechanical resistance and tablets bulk density is reported. We observe a linear relationship between densification and hardness for all four studied MOFs, with a slope being MOF-dependent. We also report conditions for improving significantly the surface over volume ratio. Finally, we evaluated our tablets stability over time in the presence of moisture.

1. Introduction

Less than 20 years after their discovery, commercial applications of Metal-Organic Frameworks (MOFs) have recently been announced.[1] We have also acknowledged in the very last years the development of pilot line production processes, such as continuous processes using water as solvent at atmospheric pressure,[2] under hydrothermal conditions,[3] or even solvent free.[4] Thanks to the demonstration of these scalable pilot lines and others, commercial applications of MOF will expand without any doubts.

Typically, synthesis processes lead to the production of MOFs as loose powders. However and except in very rare cases, applications require bodies with a specific shape such as tablets, extrudates, granulates, monoliths or coatings to cite only the most common forms. For example, in catalysis, one of the usual forms are tablets which are obtained by pressing powders. Such bodies shall present mechanical resistance to attrition and hydrostatic pressure, while preserving as much as possible the original pore structure. Bazer-Bachi *et al.* reported the catalytic conversion of vegetable oil using ZIF-8 tablets which were as active as the loose ZIF-8 powder, leading the way to further application of shaped MOFs in catalysis.[5] On the other hand, for gas storage it is utmost important to fill the storage tanks with the largest amount of adsorbent. The void fraction within the adsorbent bed is a critical factor to control in the design of an adsorbent independently of its composition or structure.[6,7] Therefore, MOFs shall be pressed into solids of high density such as tablets in order to maximize their volumetric uptake.

Despite important efforts for the development of shaping processes suitable for MOFs, challenges linked to their intrinsic fragility remain.[8] Limitations can be listed into three categories: (i) relatively low thermal stability with respect to oxides, impeding the use of classical shaping processes which are based on firing a binder-containing formulation after pelletization;[9] (ii) relatively low chemical stability in the presence of solvents, including water, making extrusion processes not generalisable;[10] (iii) relatively low mechanical stability owing to their very high porosity and flexibility, leading to structural collapsing when the applied pressure exceeds a given threshold.[11]

When taking those limitations into account, mild pelletisation by compression appears to be a practical solution for MOFs as it overcomes firing issues and the use of solvent while limiting the structural collapsing. Two review articles dealing with MOFs densification have made a quite exhaustive inventory in the field, which will not be discussed here.[12] Nevertheless, it was concluded that tablets could be obtained by compressing binderless, pure MOF powders.[13] The use of binders such as alumina, silica, graphite, or polyvinyl alcohol was also reported to reduce the structure degradation observed when even moderate strengths are applied, but they also decrease the tablets overall porosity proportionally.

The optimisation of MOFs densification consists in finding a compromise between a gain in mechanical stability of the body versus a loss of their initial properties. Ideally, structural and textural properties of the MOF crystals should be preserved while the tablets density should be as high as possible. For example, Nandasiri et al. propose an optimal tablet density of about 0.5g/cm^3 for MOF-5 and MIL-101(Cr) while maintaining their initial porosity.[14] Similar binderless densification of other MOFs among the most studied, namely ZIF-8,[5] UiO-66,[10] UiO-66-NH_2,[11,15] and HKUST-1,[5,16] have been already reported. However the tablets density increase comes with lower textural properties. This is especially the case of HKUST-1, which already collapses at modest applied pressure.

While those works pave the way to the further development of MOFs, parameters related to the shaping itself, such as the compression ramp speed and dwell time are rarely reported, while they can have a tremendous importance over the final tablets properties. More surprisingly, very few hardness tests were made although the tablets were usually reported as robust. As a result, a lack of standardization in densification studies prevents to compare mechanical stability and textural properties MOF to MOF. In addition, we may wonder whether conclusions of MOF structural stability drawn from densification data can be granted when an all-or-nothing compression type is applied.

Herein, we report a systematic study based on quantitative descriptors for the densification of UiO-66, UiO-67, UiO-66-NH_2 and HKUST-1 using a R&D tableting machine. We measured the impact of the compression step on the textural properties (namely the specific surface area and the micropore volume), the bulk density and the mechanical resistance of the resulting tablets. In contrast to the general statement claiming that HKUST-1 can hardly be densified, we show here that robust tablets of HKUST-1 can be obtained without significant degradation of its microporous structure. In addition, we have

investigated the use of low content of Expanded Natural Graphite (ENG) as a dried binder. Finally, we challenged the stability of our tablets after four months in the presence of moisture.

2. Experimental section

2.1. Synthesis of MOF powders

UiO-66 was prepared based on a protocol proposed by Kim et al.[17] A DMF solution with molar composition of zirconium chloride:terephtalic acid:hydrochloric acid = 1:1:1 was heated at 120°C for 24h under stirring. The solid product was recovered by filtration and washed twice with DMF. Remaining solvent entrapped inside the powder was exchanged first with ethanol, then with acetone, using soxhlet extraction. Finally, UiO-66 was activated under vacuum at 150°C for 12h.

UiO-67 was prepared based on a protocol proposed by Shearer et al.[18] A DMF solution with molar composition of zirconium chloride:4,4'-biphenyldicarboxylic acid:water:benzoic acid = 1:1:1.3:5 was heated at 120°C for 24h under stirring. The solid product was recovered by centrifugation, washed three times with DMF, three times with ethanol, and three times with acetone. Finally, UiO-67 was activated under vacuum at 60°C for 12h.

UiO-66-NH_2 was synthesized using the spray-drying continuous flow method.[19] A precursor suspension of 0.22M $ZrOCl_2 \cdot 8H_2O$ and 0.20M 2-aminoterephtalic acid in 24mL of a mixture of water and acetic acid (1:1) was injected into a coil flow reactor at a feed rate of 2.4mL.min^{-1} and at a temperature of 90°C. The residence time inside the coil flow reactor was 63s. The resulting pre-heated solution was then spray-dried in a Mini Spray Dryer B-290 (BÜCHI Labortechnik) at a flow rate of 336ml.min^{-1} and an inlet air temperature of 150°C, using a spray cap with a 0.5-mm-diameter hole, affording a yellow powder. This powder was then redispersed in ethanol and collected by centrifugation. The two-step washing process was repeated with acetone. The final product was dried for 12h at 60°C in air. This dried powder was finally activated under vacuum at 200°C for 6h (4°C/min temperature slope).

HKUST-1 was prepared using the spray-drying technology.[20] A solution of 0.90M $Cu(NO_3)_2 \cdot 2.5H_2O$ and 0.60M 1,3,5-benzenetricarboxylic acid in 135mL of a mixture of DMF, ethanol and water (1:1:1) was spray-dried in a Mini Spray Dryer B-290 (BÜCHI Labortechnik) at a feed rate of 4.5mL.min^{-1}, a flow rate of 336ml.min^{-1} and an inlet air temperature of 180°C, using a spray cap with a 0.5-mm-diameter hole, affording a blue powder. This powder was then redispersed in ethanol and precipitated by centrifugation. The two-step washing process was repeated with acetone. The final product was dried for 12h at 60°C in air. This dried powder was finally activated under vacuum at 150°C for 12h (4°C/min temperature slope).

2.2. Densification method and body characterization

A Medel'Pharm STYL'ONE Evolution tableting instrument was used for shaping purpose. Prior to compression, powders were deagglomerated by grinding. The die was then filled with 150mg (UiO-67), 200mg (UiO-66) or 300mg (HKUST-1, UiO-66-NH_2) of MOF powder. Punches diameter of 1.128cm were used, allowing a tableting surface of 1.00cm². The tableting press was specified a thickness to reach following a constant displacement rate, and the corresponding applied pressure was monitored. An asymmetric compression, where the penetration of the upper punch was fixed at 2mm, was used. From the moment the punches reached the powder filling height (h_0), a compression time of about 4.000ms was applied to reach the specified thickness. Then compression was hold for 400ms, before the punches went back to h_0 within 4.000ms. To avoid any residue on the internal die surface, some cellulose was pressed between two MOF tablets.

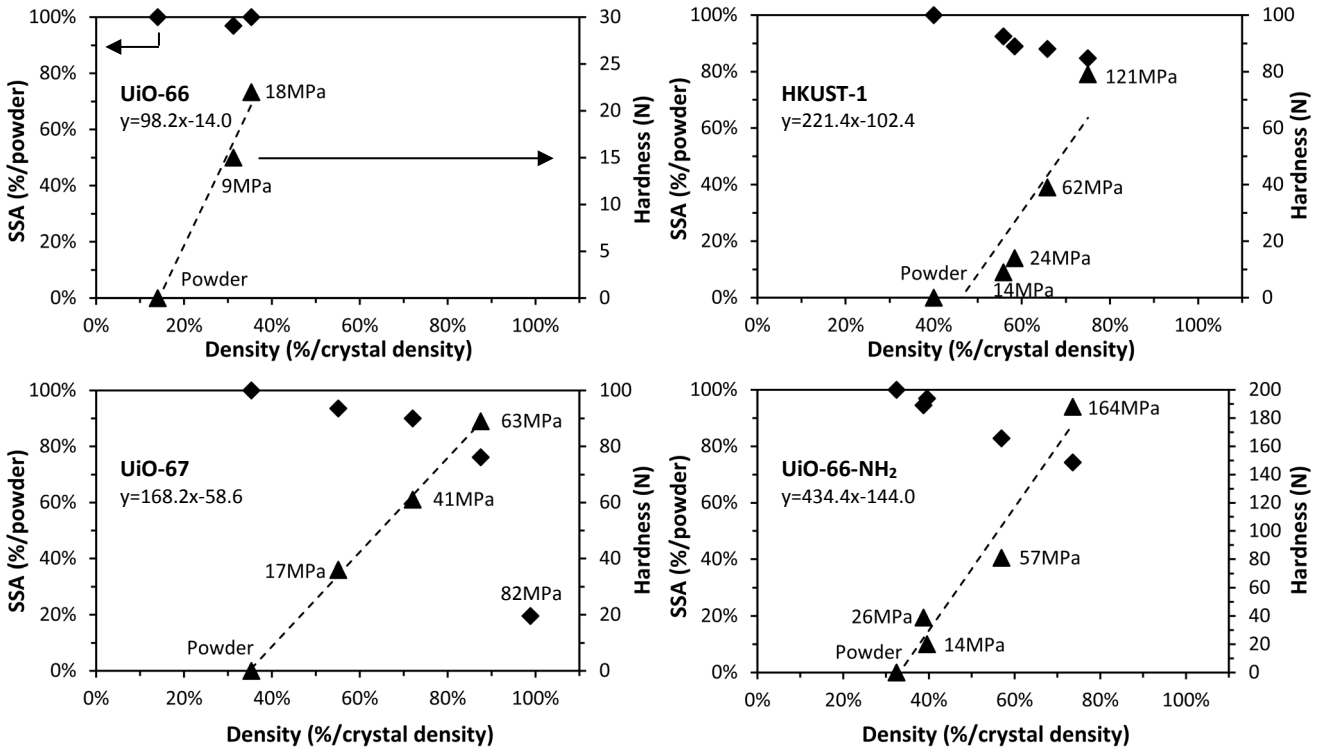

Figure 1: Impact of the degree of compression on the textural properties (rhombus) and mechanical strength (triangle) for tablets of UiO-66, HKUST-1, UiO-67 and UiO-66-NH_2. Applied pressures are indicated for each tablet, and the linear relationship hardness=f(relative density) is reported. For UiO-67, hardness was not measured above 63 MPa as the structure collapsed.

After shaping, physical parameters of MOF tablets were measured using a Pharmatron SmartTest 50. Those parameters include the weight, thickness, and diameter, allowing to calculate the tablets bulk density. The same apparatus was also used to evaluate the hardness in the transverse orientation, by pressing the side of the tablets at a constant 1mm/s displacement rate until a first load drop was detected. Such pressed tablets were usually split in two half. The degree of densification is here reported as a percentage of the crystal density which is in theory the highest density that can be achieved for a crystal. Similarly, we express the specific surface area (SSA) of the tablet as a percentage of the initial powder. The SSA is a relevant quantitative indicator, as a loss of SSA after compression indicates a partial collapse of the porous structure. Alternatively, the micropore volume can be used equally as a quantitative descriptor of the degradation of the porous networks (see **Table S1**).

The main advantage in using these indicators is that they are non dimensional, bounded between 0 and 100% and hence can be used to compare MOFs regardless of their intrinsic properties. We also provide a novel descriptor called volumetric capacity ($V_{surf.}$), which shall be especially relevant for gas storage applications. A positive effect of the shaping method is characterized by an higher volumetric surface as compared to the initial powder. Moreover, the higher this descriptor, the better the tablets shall perform for gas storage applications, until an optimum value is reached.

2.3. Structure and porosity characterization

Powder X-ray diffraction (PXRD) patterns were recorded on a Bruker D8 advance diffractometer using a CuKα radiation source and a Lynx-Eye detector. Nitrogen adsorption isotherms were measured at 77K on a BELSORP-mini device from BEL Japan. Samples were outgassed at 150°C overnight prior to measurement. Specific surface areas (SSA) were determined using the BET method. The micropore volume ($V_{micro.}$) was evaluated from the adsorbed volume of N_2 at P/P_0=0.3. In order to calculate the bulk density of tablets, dry masses were estimated from Thermogravimetric (TG) analyses measured on a Mettler Toledo TGA-DSC1 using reconstituted air (**Figure S1 and Table S2**). Linker defects was also evaluated from TGA, supposing that the remaining weight at 800°C corresponds to the metal oxide, namely ZrO_2 (UiO-) or CuO (HKUST-1). This allows to determine directly the weight of a theoretical dehydroxylated MOF structure Zr_6O_6(linker)$_6$ and Cu_3BTC_2, which is compared to the experimental remaining weight after solvent loss and dehydroxylation (taking into account metal oxidation). The weight difference is thus assigned to linker defects. This method doesn't take into account possible cluster defects. Powders bulk density, also called tap density, was determined by adding a known mass of deagglomerated MOF powder into a vial with high height/diameter ratio. Then, the vial was repetitively hit on a hard surface until no more volume change could be observed -generally a few hundred times-, thus allowing to measure the packed bed dimensions. Scanning electron microscopy (SEM) was made on a Hitachi S-4800

Table 1: Textural properties and resulting volumetric surface of optimized MOF tablets.

MOF	Form	Applied pressure (MPa)	SSA (m^2/g)	$V_{micro.}$ (cm^3/g)	Crystal density (g/cm^3)	Bulk density (g/cm^3)	Hardness (N)	$V_{surf.}$ (m^2/cm^3)
UiO-66	Powder	-	1426	0.54	1.21	0.17	-	242
	Tablet	18	1459	0.54		0.43	22	627
UiO-66-NH_2	Powder	-	839	0.34	1.26	0.41	-	344
	Tablet	164	625	0.25		0.93	188	581
UiO-67	Powder	-	2034	0.90	0.71	0.25	-	509
	Tablet	63	1549	0.70		0.62	89	960
HKUST-1	Powder	-	1288	0.49	1.20	0.48	-	618
	Tablet	121	1091	0.40		0.90	79	982

3. Results and discussion

3.1. Influence of compression on MOFs tablets properties

The impact of the densification step on the final tablet properties including density, SSA and hardness is presented in **Figure 1**. First, we can see that the tap densities of MOF powders are very low with respect to their corresponding crystal density: it is only 14% for UiO-66, and the highest value is for HKUST-1 with a relative density of 40%. We can also note that while being isostructural to UiO-66, UiO-66-NH_2 tap density reaches 32% of its crystal density. Here, the difference between those two isostructural MOFs is partly due to the synthesis protocol.

MOF tablets were observed by SEM and images are presented in Supporting Information. Small and rounded crystals of HKUST-1 (**Fig.S2**) and UiO-66-NH_2 (**Fig.S3**) are observed. No large agglomerate such as usually produced by spray-drying can be seen,[19,20] meaning that grinding was successful for deagglomeration. UiO-67 prepared by a solvothermal method leads to micrometric crystals with a bipyramidal shape (**Fig.S4**). This latter is typical of the isostructural Zr-based series. While also part of this series, UiO-66 crystals are small and rounded (**Fig.S5**). This is however in accordance with previous results.[17] Moreover, SEM clichés reveal that densification occurs more notably at the surface in contact with the punches.

For all studied MOFs, compression can yield tablets with twice higher density than their corresponding powders, while preserving more than 70% of the initial SSA. For instance HKUST-1, which has a reputation of being fragile, was densified to 75% of its crystal density while preserving 85% of its initial textural properties when pressed at 121MPa. One may note that the densest random packing of spheres is about 64 to 74% of the three-dimensional volume.[21] Surprisingly, we achieved here comparable values while limiting the textural properties loss.

As expected, the highest the applied pressure, the highest the achieved densification. More interestingly, we observe a linear relationship between densification and hardness for all four studied MOFs below 80% of relative density, with a slope being MOF-dependent. To the best of our knowledge it is the first time that this behaviour is reported.

Obviously the densification level or the hardness cannot be enhanced by an ever increasing applied pressure without leading to a porous structure collapse. When the highest density is sought, the loss of microporosity shall be as reduced as possible, otherwise affecting the tablets ultimate performances. For UiO-66, no loss of SSA has been observed until 40% of relative density which is the highest level we have investigated as the aim was to reach a hardness high enough for further production of grains. It does not preclude that higher level of densification cannot be obtained without damaging the porous structure. For other studied MOFs, a modest but somehow linear decrease can be observed with increasing densification. Again, the decreasing rate is MOF-dependent.

Zr-based MOFs are known for their high mechanical and thermal stability owing to their 12-fold connected clusters in the three spatial directions.[22,23] This stability can be compromised by the number of missing linkers per node -usually about 2-,[24,25] however the addition of monocarboxylic acids during synthesis of UiO-66 proved to enhance its stability.[26] UiO-66 and UiO-67 powders prepared by solvothermal synthesis present 17% of missing linkers per node (2 out of 12), which is comparable to the literature data.[25,27] Although that UiO-67 possesses the same topology than UiO-66 and the same degree of defects, its mechanical stability under compression is relatively modest as the porous structure collapses between 63 and 82MPa (SSA loss of about 80%). This is in line with prior studies.[25,28] Here, we can safely assume that the reason of this collapsing is due to the very high densification degree already reached, beyond 90%, coupled with the very low flexibility of the framework.[29]

In summary, when MOF powders are pressed into tablets, up to a two-fold bulk density can be achieved at the expense of slightly reduced textural properties. For the production of MOF grains for catalysis, where a maximal gravimetric uptake is expected, one might press a tablet only to reach a hardness above 10N which is an usual industrial target,[30] thus limiting SSA loss. This hardness value is easily surpassed by applying pressures below 50MPa in the case of all the binderless MOF tablets studied here.

In the case of gas storage and without precluding neither a specific gas nor application conditions, we can foresee that the densification level which would offer the greatest surface area per unit of volume should perform better assuming mainly Van der Waals type interactions. We have calculated the volumetric capacity descriptor by multiplying the tablets microporous volume by their bulk density. This descriptor $V_{surf.}$, presented in **Table 1**, is expressed in cubic centimetre per cubic centimetre (m^2/cm^3). It can be pointed out that the microporous volume is correlated to the specific surface area and as consequence either one or the other can be used as descriptors (SI). Detailed inputs for all tablets can be found in **Table S2**. One may note that in most cases (HKUST-1, UiO-66, UiO-66-NH_2), the

"optimized" tablet is the one compressed at the highest pressure, meaning that optimal pressure might not have been reached here and the volumetric surface could still be increased. This is especially the case of UiO-66, which is likely to resist to compression pressures up to 2.500MPa with 50% of the initial SSA maintained.[10] Nevertheless, a remarkable increase of tablets volumetric surface can already be observed as compared to their powders counterpart, from 1.6 to 2.5-fold. For example, the volumetric surface area of HKUST-1 can be increased from 618 to 982m²/cm³. According to calculations made by Daily et al.,[7] such densified HKUST-1 tablets could result in an outperforming adsorbed natural gas (ANG) adsorbent.

3.2. Comparison with literature data

Our results were further compared to the literature state-of-the-art in **Figure 2**. For UiO-66 and UiO-66-NH_2, we can see that the loss of SSA as function of the applied pressure is well in line with the literature data.[12,13]

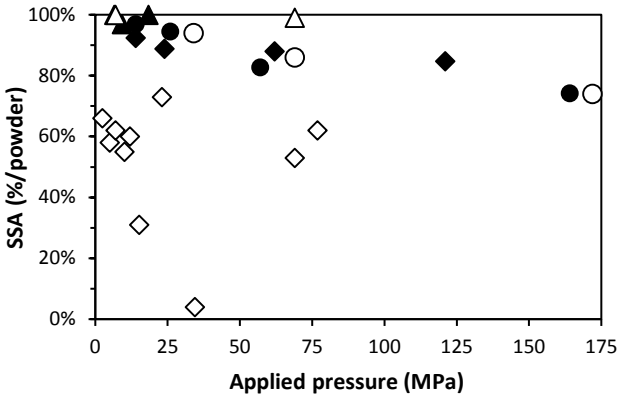

Figure 2: SSA loss during compression observed in this work (black) and reported in the literature (white), using UiO-66 (triangle), UiO-66-NH_2 (round) and HKUST-1 (rhombus) powders.[10,15,16]

However, important discrepancies are observed in the case of HKUST-1. Herein up to 85% of the original SSA of the powder was preserved at a moderate pressure of 120MPa, while about 50% of SSA loss was reported at lower pressures of 10 and 70MPa elsewhere.[16] This could arise from several factors: **(1)** we used a relatively slow pressure increase rate, which could allow HKUST-1 crystals to rearrange during compression ; **(2)** as shown on **Figure 3**, solvent presence within the framework during compression allows maintaining its integrity, while in the literature HKUST-1 powders are typically activated prior to compression ; **(3)** presence of defects within a MOF structure is likely to fragilize its resistance during compression. Here, assuming that there is no cluster defect, the HKUST-1 powder used only presents 10% of linker defects as presented in **Table S2**. The latter assumption can hardly be verified as it would require shaping exactly the same powders that were used elsewhere. One may note that in the literature, the mechanical resilience of zeolithic MOFs single crystals was greatly improved using common solvents, namely ethanol and butanol.[31]

Figure 3: Nitrogen adsorption isotherms of as-made HKUST-1 powder (black/top), and HKUST-1 tablets pressed at 62MPa with as-made powder (blue/middle) or with powder fully activated prior compression (red/bottom).

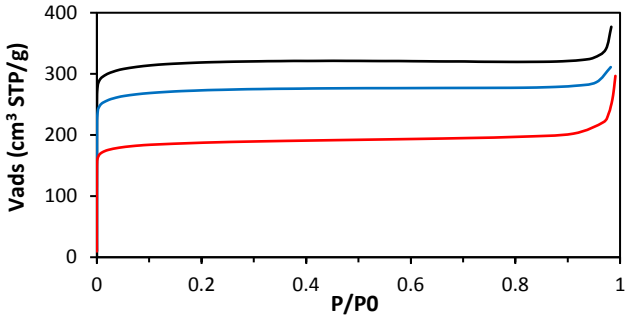

3.3. Addition of Expanded Natural Graphite as binder for HKUST-1 powder

Graphite is generally used as an additive for improving materials thermal conductivity.[32] Graphite was also applied as a mineral binder with UiO-66.[33] Herein, up to 2wt% of expanded natural graphite was mixed with HKUST-1 powder prior to compression, and its impact on both the textural properties and the hardness of the resulting tablet was investigated and presented in **Figure 4**.

No measurable impact on the SSA could be observed at any of the applied pressure, while a minor enhancement of the hardness of about 7N can be noted with 2wt% ENG, almost independently of the applied pressure. This latter observation is particularly interesting for shaping MOFs at low pressure, thus maximizing the textural properties while reaching a hardness high enough for applications.

Figure 4: Impact of compression on SSA (according to initial powder) and hardness of pure HKUST-1 tablets (white), or HKUST-1 mixed with 1wt% graphite (grey) and 2wt% graphite (black). Circles represent the SSA (according to initial powder),

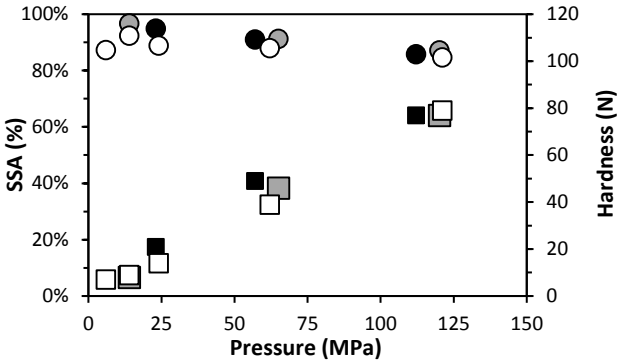

and squares represent the hardness.

3.4. Overtime ageing of tablets in polyethylene bag

After characterization, each tablet was sealed in a small polyethylene bag and left on the shelf under room conditions. It shall be pointed out that PE bags are not impermeable. Indeed, the permeability to humidity for example is 0.16g/m2/day (REF) sinon ..from to astm measurements. The packaging in PE bags does not prevent gas exchanges but limit

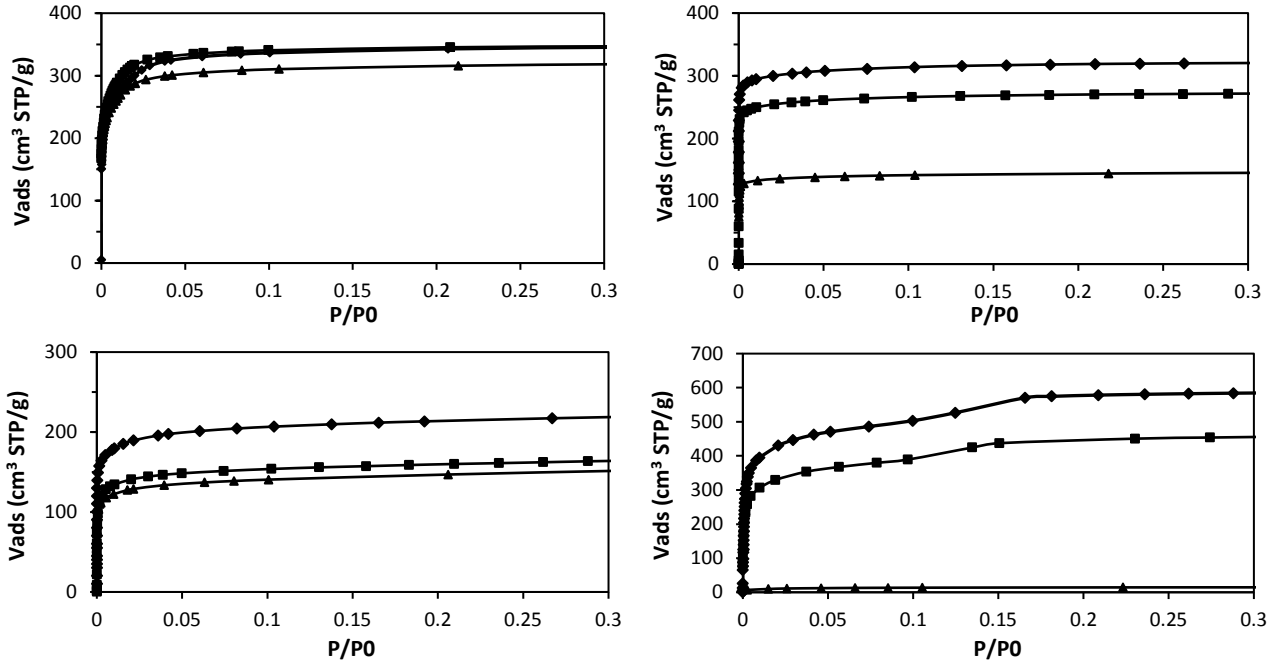

Figure 5: Nitrogen adsorption isotherms measured on UiO-66 (top-left), UiO-66-NH_2 (bottom-left), HKUST-1 (top-right) and UiO-67 (bottom-right): activated powders (rhombus), as-made tablets (square) and tablets aged for 4 months at standard room conditions (triangle).

the exchange rates. The tablets with optimised volumetric capacity were then characterized again four months later in order to check their stability in the presence of moisture. Nitrogen adsorption isotherms of the different tablets are shown on **Figure 5** and their textural properties are summarized in **Table 2**. In the case of UiO-66 and UiO-66-NH_2, only a slight decrease of SSA and micropore volume was observed (-9 to -11%), while the PXRD was unchanged as shown in **Figure S6**.

In contrast, for UiO-67 tablets, 96% of their initial SSA was lost after 4 months. Notably, PXRD patterns shown on **Figure S7** confirm a striking loss of crystallinity. It was shown that UiO-67 is poorly stable in humid conditions.[34] However, contrarily to what was published by DeCoste et al.,[34] no monoclinic zirconia diffraction peak could be observed: the degraded product can still be identified as pure UiO-67. This result confirms that UiO-67 cannot be used in processes where even traces of water are present.

HKUST-1 stability over time was extensively studied as it is one of the best candidates for gas storage and chromatography stationary phase.[35] Todaro et al. investigated HKUST-1 decomposition process with air moisture.[36] They concluded that Cu-O bonds hydrolysis is driven by the accumulation of water molecules during exposure. This phenomenon is reversible for short exposure times, up to 20 days, following a simple vacuum treatment. For longer exposition times, irreversible hydrolysis occurs. However, this hydrolysis is limited as in their case up to 60% of the initial SSA is still preserved after 188 days. Interestingly, our HKUST-1 tablets aged similarly, with 53% of their initial SSA retained after 4 months. We can deduce that irreversible hydrolysis also occurred after tableting. Therefore, shaping MOF powders into dense tablets does not improve significantly their resistance toward air moisture. One can suppose that the formation of a dense crust of MOFs during tableting slows down the diffusion of moisture within the tablets at first, but does not prevent the degradation.

Conclusions

We present here a general methodology for comparing the impact of MOF powders compression on their textural and mechanical properties using non dimensional indicators. By compression, the tablets bulk density can be increased by 1.8 to 3.4-fold while the specific surface area decrease is comprised between 0 and 30% for all MOFs studied here. We report here for the first time that the mechanical stability deduced from hardness tests is proportional to the bulk density, both being MOF-dependent.

In contrast to all past densification studies made on HKUST-1, we demonstrated that robust tablets presenting only limited textural degradation can be obtained. We believe that it arises at least partly from our compression protocol, where the compression rate and dwell time are thoroughly controlled. As a consequence, densification results obtained by un-controlled or poorly-controlled manner such as when using a manual press shall be interpreted with care. Moreover, as reported in the case of ZMOFs single cystals, the presence of solvent traces within the HKUST-1 porosity seems beneficial during compression.

We pinpointed here that depending on the final application, namely catalysis or gas storage, a different strategy can be used. For catalysis a mild pressure, usually around 20MPa, seems enough to produce tough and highly porous tablets that can then be grinded and sieved. The use of graphite up to 2wt% can also be beneficial as it lowers the pressure required to reach a certain hardness, thus maximizing the retained textural properties. For gas storage, the maximum volumetric surface

was obtained at the highest applied pressure, excepted for UiO-67 which collapses at 82 MPa. However, only UiO-66 and UiO-66-NH_2 proved to be stable over time in the presence of moisture, making them highly attractive for further production and application.

Acknowledgements

This work has been carried out within the ProDIA project that has received funding from the *European Union's Horizon 2020 research and innovation programme* under grant agreement No 685727. We would like to thank S. Nieto Bobadilla and T. Menard from Medel'Pharm (FR) for the expertise provided, Didier Cot for the SEM images, and Coldway (FR) for providing enhanced natural graphite.

References

1 Editorial, *Nature Chem.*, 2016, **8**, 987.
2 M. Rubio-Martinez, T.D. Hadley, M.P. Batten, K.-C. Carey, T. Barton, D. Marley, A. Mönch, K.-S. Lim and M.R. Hill, *ChemSusChem*, 2016, **9**, 1; H. Reinsch, S. Waitschat, S.M. Chavan, K.P. Lilerud and N. Stock, *Eur. J. Inorg. Chem.*, 2016, **27**, 4490.
3 A.S. Munn, P.W. Dunne, S.V.Y. Tang and E.H. Lester, *Chem. Commun.*, 2015, **51**, 12811.
4 D. Crawford, J. Casaban, R. Haydon, N. Giri, T. McNally and S.L. James, *Chem. Sci.*, 2015, **6**, 1645.
5 D. Bazer-Bachi, L. Assié, V. Lecocq, B. Harbuzaru and V. Falk, *Powder Technol.*, 2014, **255**, 52.
6 H.C. Foley and A. Qajar, *Ind. Eng. Chem. Res.*, 2014, **53**, 19649.
7 M. Beckner and A. Dailly, *Appl. Energy*, 2015, **149**, 69; M. Beckner and A. Dailly, *Appl. Energy*, 2016, **162**, 506.
8 A.I. Spjelkavik, A. Sevilime, S. Divekar, T. Didriksen and R. Blom, Chem. Eur. J., 2014, 20, 8973; B. Böhringer, R. Fischer, M.R. Lohe, M. Rose, S. Kaskel and P. Küsgens (2011) MOF Shaping and Immobilization, in Metal-Organic Frameworks: Applications from Catalysis to Gas Storage (ed D. Farrusseng), Wiley-VCH Verlag GmbH & Co. KGaA, Weinheim, Germany.
9 S. Mitchell, N.-L. Michels and J. Pérez-Ramírez, *Chem. Soc. Rev.*, 2013, **42**, 6094; G.T. Whiting, A.D. Chowdhury, R. Oord, P. Paalanen, B.M. Weckhuysen, *Faraday Discuss.*, 2016, **188**, 369.
10 P.S. Bárcia, D. Guimarães, P.A.P. Mendes, J.A.C. Silva, V. Guillerm, H. Chevreau, C. Serre and A.E. Rodrigues, *Micro. Meso. Mater.*, 2011, **139**, 67; G.W. Peterson, J.B. DeCoste, T.G. Glover, Y. Huang, H. Jasuja and K.S. Walton, *Micro. Meso. Mater.*, 2013, **179**, 48.
11 P.G. Yot, K. Yang, F. Ragon, V. Dmitriev, T. Devic, P. Horcajada, C. Serre and G. Maurin, *Dalton Trans.*, 2016, **45**, 4283.
12 F. Akhtar, L. Andersson, S. Ogunwumi, N. Hedin and L. Bergström, *J. Eur. Ceram. Soc.*, 2014, **34**, 1643; S.C. McKellar and S.A. Moggach, *Acta Cryst.*, 2015, B71.
13 K.W. Chapman, G.J. Halder and P.J. Chupas, *J. Am. Chem. Soc.*, 2009, **131**, 17546; M.A. Moreira, J.C. Santos, A.F.P. Ferreira, J.M. Loureiro, F. Ragon, P. Horcajda, K.-E. Shim, Y.-K. Hwang, U.-H. Lee, J.-S. Chang, C. Serre and A.E. Rodrigues, *Langmuir*, 2012, **28**, 5715; D. Peralta, G. Chaplais, A. Simon-Masseron, K. Barthelet and G.D. Pirngruber, *Ind. Eng. Chem. Res.*, 2012, **51**, 4692; R. Zacharia, D. Cossement, L. Lafi and R. Chahine, *J. Mater. Chem.*, 2010, **20**, 2145.
14 M.I. Nandasiri, S.R. Jambovane, B.P. McGrail, H.T. Schaef and S.K. Nune, *Coord. Chem. Rev.*, 2016, **311**, 38.
15 G.W. Peterson, J.B. DeCoste, F. Fatollahi-Fard and D.K. Britt, *Ind. Eng. Chem. Res.*, 2014, **53**, 701.
16 J. Kim, S.-H. Kim, S.-T. Yang and W.-S. Ahn, *Micro. Meso. Mater.*, 2012, **161**, 48; J. Liu, P.K. Thallapally and D. Strachan, *Langmuir*, 2012, **28**, 11584.
17 S.-N. Kim, Y.-R. Lee, S.-H. Hong, M.-S. Jang and W.-S. Ahn, *Catal. Today*, 2015, **245**, 54.
18 G.C. Shearer, S. Forselv, S. Chavan, S. Bordiga, K. Mathisen, M. Bjørgen, S. Svelle and K.-P. Lillerud, *Top. Catal.*, 2013, **56**, 770.
19 L. Garzón-Tovar, M.Cano-Sarabia, A. Carné-Sánchez, C. Carbonell, I. Imaz and D. Maspoch, *React. Chem. Eng.*, 2016, **1**, 533.
20 A. Carné-Sánchez, I. Imaz, M. Cano-Sarabia and D. Maspoch, *Nature Chem.*, 2013, **5**, 203.
21 J.R. Parrish, Nature, 1961, 190, 800.
22 L. Valenzano, B. Civalleri, S. Chavan, S. Bordiga, M.H. Nilsen, S. Jakobsen, K.P. Lillerud and C. Lamberti, *Chem. Mater.*, 2011, **23**, 1700.
23 Kandiah, M.H. Nilsen, S. Usseglio, S. Jakobsen, U. Olsbye, M. Tilset, C. Larabi, E.A. Quadrelli, F. Bonino and K.-P. Lillerud, *Chem. Mater.*, 2010, **22**, 6632; Y. Bai, Y. Dou, L.-H. Xie, W. Rutledge, J.-R. Li and H.-C. Zhou, *Chem. Soc. Rev.*, 2016, **45**, 2327.
24 G.C. Shearer, S. Chavan, J. Ethiraj, J.G. Vitillo, S. Svelle, U. Olsbye, C. Lamberti, S. Bordiga and K.P. Lillerud, *Chem. Mater.*, 2014, **26**, 4068.
25 S.M.J. Rogge, J. Wieme, L. Vanduyfhuys, S. Vandenbrande, G. Maurin, T. Verstraelen, M. Waroquier and V.. Speybroeck, *Chem. Mater.*, 2016, **28**, 5721.
26 B. Van de Voorde, I. Stassen, B. Bueken, F. Vermoortele, D. De Vos, R. Ameloot, J.-C. Tan and T.D. Bennett, *J. Mater. Chem. A*, 2015, **3**, 1737.
27 M.J. Katz, Z.J. Brown, Y.J. Colón, P.W. Siu, K.A. Scheidt, R.Q. Snurr, J. Hupp and O. Farha, Chem. Commun., 2013, 49, 9449.
28 H. Wu, T. Yildirim and W. Zhou, *J. Phys. Chem. Lett.*, 2013, **4**, 925.
29 C.L. Hobday, R.J. Marshall, C.F. Murphie, J. Sotelo, T. Richards, D.R. Allan, T. Düren, F.-X. Coudert, R.S. Forgan, C.A. Morrison and S.A. Moggach, *Angew. Chem. Int. Ed.*, 2016, **55**, 2401.
30 N.-L. Michels, S. Mitchell, M. Milina, K. Kunze, F. Krumeich, F. Marone, M. Erdmann, M. Marti and J. Pérez-Ramírez, *Adv. Funct. Mater.*, 2012, **22**, 2509.
31 T.D. Bennett, J. Sotelo, J.-C. Tan and S.A. Moggach, CrystEngComm, 2015, 17, 286.
32 D. Liu, J.J. Purewal, J. Yang, A. Sudik, S. Maurer, U. Mueller, J. Ni and D.J. Siegel, *J. Hydrogen Energy*, 2012, **37**, 6109.
33 M.A. Moreira, J.C. Santos, A.F.P. Ferreira, J.M. Loureiro, F. Ragon, P. Horcajda, K.-E. Shim, Y.-K. Hwang, U.-H. Lee, J.-S. Chang, C. Serre and A.E. Rodrigues, *Langmuir*, 2012, **28**, 5715.
34 J.B. DeCoste, G.W. Peterson, H. Jasuja, T.G. Glover, Y.-G. Huang and K.S. Walton, *J. Mater. Chem. A*, 2013, **1**, 5642.
35 M.S. Singh, N.R. Dhumal, H.J. Kim, J.Kiefer and J.A. Anderson, *J. Phys. Chem. C*, 2016, **120**, 17323.
36 M. Todaro, G. Buscarino, L. Sciortino, A. Alessi, F. Messina, M. Taddei, M. Ranocchiari, M. Cannas and F.M. Gelardi, *J. Phys. Chem. C*, 2016, **120**, 12879.